Rational Design, Synthesis, and Crystallographic Analysis of a Hydroxyethylene-Based HIV-1 Protease Inhibitor Containing a Heterocyclic P_1'-P_2' Amide Bond Isostere†

Scott K. Thompson,*,§ Krishna H. M. Murthy,‖,▽ Baoguang Zhao,‖ Evon Winborne,‖ David W. Green,⊥,‡ Seth M. Fisher,⊥ Renee L. DesJarlais,# Thaddeus A. Tomaszek, Jr.,§ Thomas D. Meek,§,‡ John G. Gleason,§ and Sherin S. Abdel-Meguid*,‖

Departments of Medicinal Chemistry, Macromolecular Sciences, Protein Biochemistry, and Physical and Structural Chemistry, SmithKline Beecham Pharmaceuticals, King of Prussia, Pennsylvania 19406

Received May 20, 1994®

The rational design and synthesis of a highly potent inhibitor of HIV-1 protease have been accomplished. The inhibitor, SB 206343, is based on a model derived from the structure of the MVT-101/HIV-1 protease complex and contains a 4(5)-acylimidazole ring as an isosteric replacement for the P_1'-P_2' amide bond. It is a competitive inhibitor with an apparent inhibition constant of 0.6 nM at pH 6.0. The three-dimensional structure of SB 206343 bound in the active site of HIV-1 protease has been determined at 2.3 Å resolution by X-ray diffraction techniques and refined to a crystallographic discrepancy factor, R ($=\sum||F_o| - |F_d||/\sum|F_o|$), of 0.194. The inhibitor is held in the enzyme by a set of hydrophobic and polar interactions. N-3 of the imidazole ring participates in a novel hydrogen-bonding interaction with the bound water molecule, demonstrating the effectiveness of the imidazole ring as an isosteric replacement for the P_1'-P_2' amide bond in hydroxyethylene-based HIV-1 protease inhibitors. Also present are hydrogen-bonding interactions between N-1 of the imidazole ring and the carbonyl of Gly-127 as well as between the imidazole acyl carbonyl oxygen and the amide nitrogen of Asp-129, exemplifying the peptidomimetic nature of the 4(5)-acylimidazole isostere. All of these interactions are in qualitative agreement with those predicted by the model.

Introduction

Human immunodeficiency virus type-1 (HIV-1), a member of the Retroviridae family, is the causative agent of acquired immunodeficiency syndrome (AIDS).[1,2] A crucial step in the replicative cycle of the virus involves the processing by a virus-encoded protease of the viral *gag* and *gag-pol* polyproteins into structural proteins and enzymes essential for the proper assembly and maturation of fully infectious virions.[3,4] The HIV-1 protease is therefore an attractive target for the design of antiviral agents for the treatment of AIDS.

The HIV-1 protease is a homodimeric enzyme consisting of two 99-amino acid polypeptides and is classified as an aspartyl protease on the basis of active site sequence similarity[5,6] and structural analogy to the previously characterized monomeric aspartic proteases renin, pepsin, endothiapepsin, penicillopepsin, and rhizopuspepsin.[7] Structurally, the enzyme is predominantly composed of β-strands and the active site containing two aspartyl residues is formed at the dimer interface with each monomer contributing one residue, as has been verified by crystallographic analysis of recombinant and synthetic forms of HIV-1 protease.[8-10] The protease also contains two flexible extended β-hairpin structures, or so-called "flaps", which upon binding of a ligand undergo movements of up to 7 Å at the tips to tightly embrace the ligand. This phenomenon has been observed extensively in X-ray crystal structures of HIV-1,[11] HIV-2,[12,13] and SIV[14,15] protease/inhibitor complexes.

The design of inhibitors of HIV-1 protease has met with much success in the recent past, owing greatly to the availability of crystallographic data from enzyme/inhibitor complexes. With the exception of a recently reported series of C_2 symmetric cyclic ureas,[16] these inhibitors are peptide analogs in which the scissile amide bond has been replaced by a nonhydrolyzable isostere: for example, peptides containing statine, secondary amines, hydroxyethylenes, hydroxyethylamines, 1,2-diols, and ketones.[17,18] Additionally, pseudosymmetric[19,20] and C_2 symmetric[16,21] inhibitors which take advantage of the C_2 symmetric nature of the enzyme have been reported. Each of these classes has provided extremely potent compounds that inhibit HIV-1 protease in the nanomolar and sub-nanomolar range and are also quite effective as inhibitors of HIV-1 replication in cell cultures.[19,22-25] However, most of these inhibitors are peptide-based and although the scissile amide bond has been replaced with an isostere, they still contain a number of labile amide bonds. We sought to design an improved antiviral drug by replacement of one or more additional amide bonds with isosteres that are more hydrolytically stable and may be conducive to improved transport.[26] We took as our approach the substitution of such an isostere for the P_1'-P_2' (nomenclature of Schechter and Berger[27]) amide bond.

The development of an isostere for the P_1'-P_2' amide bond presents a formidable challenge within the context of inhibition of HIV-1 protease. Not only must the isostere provide the correct *trans* orientation about the

† The refined coordinates for the complex have been deposited in the Protein Data Bank under the file name 2HOS.

§ Department of Medicinal Chemistry.

‖ Department of Macromolecular Sciences.

▽ Present address: Fels Institute for Cancer Research and Molecular Biology, 3307 N. Broad St., Philadelphia, PA 19140.

⊥ Department of Protein Biochemistry.

‡ Present address: Department of Cardiovascular Biochemistry, Bristol-Myers Squibb Pharmaceutical Research Institute, Princeton, NJ 08453-4000.

Department of Physical and Structural Chemistry.

® Abstract published in *Advance ACS Abstracts*, August 1, 1994.

0022-2623/94/1837-3100$04.50/0

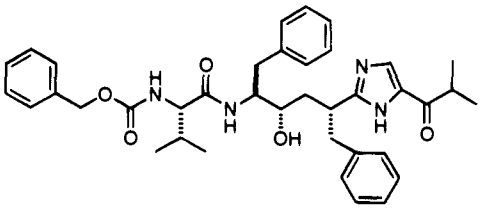

1
(SB206343)

Figure 1. HIV-1 protease inhibitor SB 206343 (**1**).

amide bond portion of the isostere but it must be capable of functioning as both a hydrogen bond acceptor for the bound water molecule and a hydrogen bond donor to the carbonyl oxygen of Gly-27. Bearing in mind that the isostere must also be hydrolytically stable, an imidazole ring appeared to be a promising candidate.[28] Using the X-ray crystal structure of the MVT-101/HIV-1 protease complex[29] as a template, a model was constructed of a hydroxyethylene-based inhibitor that contained an imidazole ring as a replacement for the P_1'—P_2' amide bond and showed an excellent geometry for the formation of a hydrogen bond from the imidazole nitrogen to the bound water molecule, as well as for the extension of the backbone structure from the 5-position of the imidazole. The present report describes the rational design and synthesis of a highly potent, imidazole-containing inhibitor of HIV-1 protease, SB 206343 (**1**; Figure 1), and its three-dimensional structure bound in the active site of the enzyme. Analysis of the structure of this complex and comparison with structures of other HIV-1 protease/inhibitor complexes has validated the effectiveness of this isostere as a replacement for the P_1'—P_2' amide bond in the context of HIV-1 protease inhibition.

Results and Discussion

Inhibitor Synthesis. SB 206343 and its analogs were prepared from the known (2*R*,4*S*,5*S*)-2-benzyl-5-[(*tert*-butoxycarbonyl)amino]-4-(*tert*-butyldimethylsiloxy)-6-phenylhexanoic acid (**2**)[30] as shown in Scheme 1. EDCl-promoted coupling of **2** with 4-aminoisoxazoles **3** and **4**[31] provided *N*-(4-isoxazolyl)amides **5** and **6**, which were then subjected to hydrogenolysis followed by base-catalyzed cyclization to afford 4(5)-acylimidazoles **7** and **8**, respectively. Deprotection of the *tert*-butyldimethylsilyl ethers provided compounds **9** and **10**. Alternatively, a greater diversity of acyl substitution was incorporated by addition of Grignard reagents to aldehyde **7** followed by oxidation of the resulting secondary alcohols **11**—**14** with manganese dioxide[32] and subsequent deprotection of the *tert*-butyldimethylsilyl ethers to provide compounds **15**—**18**. Finally, removal of the *tert*-butyl carbamate from **17** with trifluoroacetic acid followed by EDCl-promoted coupling of the resulting primary amine with N-Cbz-L-valine provided SB 206343 (**1**). In an effort to investigate the effect of the basicity of the imidazole on HIV-1 protease inhibition, two reduced 4(5)-acylimidazoles, **19** and **20**, were prepared as mixtures of diasteromers (Scheme 2). Reduction of 4(5)-acetylimidazole **10** with sodium borohydride provided diols **19**, while diols **20** were prepared by deprotection of *tert*-butyldimethylsilyl ether **13**.

Inhibition of HIV-1 Protease. The inhibitors incorporating the 4(5)-acylimidazole isostere exhibited apparent inhibition constants in the range of 0.6—3500 nM (Table 2). An investigation of the effect of the size of the acyl substituent on the imidazole ring has revealed that inhibition increases with increasing size of the substituent with the apparent optimal size being that of propionyl or 2-methylpropionyl (compounds **15** and **17**, respectively). Inhibitory potency decreases with acyl substituents more bulky than 2-methylpropionyl (compound **18**). These structure—activity data support the concept that the alkyl portion of the acyl substituent binds in the hydrophobic S_2' subsite of the enzyme, as is observed in the structure of the SB 206343/HIV-1 protease complex (*vide infra*). Additionally, replacement of the N-terminal Boc group with an N-Cbz-valine residue results in a 150-fold increase in inhibitory potency (SB 206343). These inhibition constants compare favorably to those of hydroxyethylene-based inhibitors containing peptide bonds in place of the isosteric imidazole ring (final two entries in Table 2). It is noteworthy that reduction of the acyl functionality in these inhibitors to produce 4(5)-(1-hydroxyalkyl)imidazoles results in a 30—40-fold decrease in inhibitory potency (compounds **19** and **20**). The replacement of an acyl substituent on a heterocycle with an alkyl group is expected to significantly decrease the acidity of the ring and therefore make it a stronger hydrogen bond acceptor. This transformation when applied to acetylimidazole **10** results in a loss in acidity of three pK_a units (pK_a = 3.7 for compound **10** vs 6.7 for entry **19**). Since the assay is conducted at pH 6, we believe this decrease in activity upon decrease in ring acidity to be partially a result of protonation of the ring at the assay pH, which would eliminate its hydrogen bond-accepting capability. Consistent with this hypothesis is the fact that the 4(5)-(1-hydroxyethyl)imidazole **19** exhibits pH-dependent inhibition of HIV-1 protease, with inhibition decreasing dramatically at pH values below the pK_a cited above. An alternative explanation for this decrease in activity may reside in the departure of the hydroxyl group α to the imidazole ring in compounds **19** and **20** from the optimal orientation for the formation of a hydrogen bond to the Asp-129 backbone NH or in a global conformational change in the inhibitor brought about by the presence of this additional hydroxyl group.

Table 1. Refinement Statistics

R-factor[a]	0.194
resolution range (Å)	6.0—2.3
no. of reflections	7142
no. of protein atoms	1520
no. of inhibitor atoms	94
no. of solvent molecules	15
rms deviations from ideal values	
bond lengths (Å)	0.019
bond angles (degree)	3.86

[a] R-factor = $\Sigma||F_o| - |F_c||/\Sigma|F_o|$, where $|F_o|$ and $|F_c|$ are the observed and calculated structure factor amplitudes, respectively.

Crystallographic Refinement of the Structure. The statistics listed in Table 1 are consistent with a well-refined structure within the limits of precision and resolution of the measured data. As in previous studies of HIV-1 protease complexed with asymmetric inhibitors[33,34] and with a C_2 symmetric inhibitor,[20,35] we observed two distinct orientations of the inhibitor related to each other by the pseudo-2-fold axis of the enzyme dimer, each oirentation present at half-occupancy in the crystal lattice. When refinement of the

Scheme 1

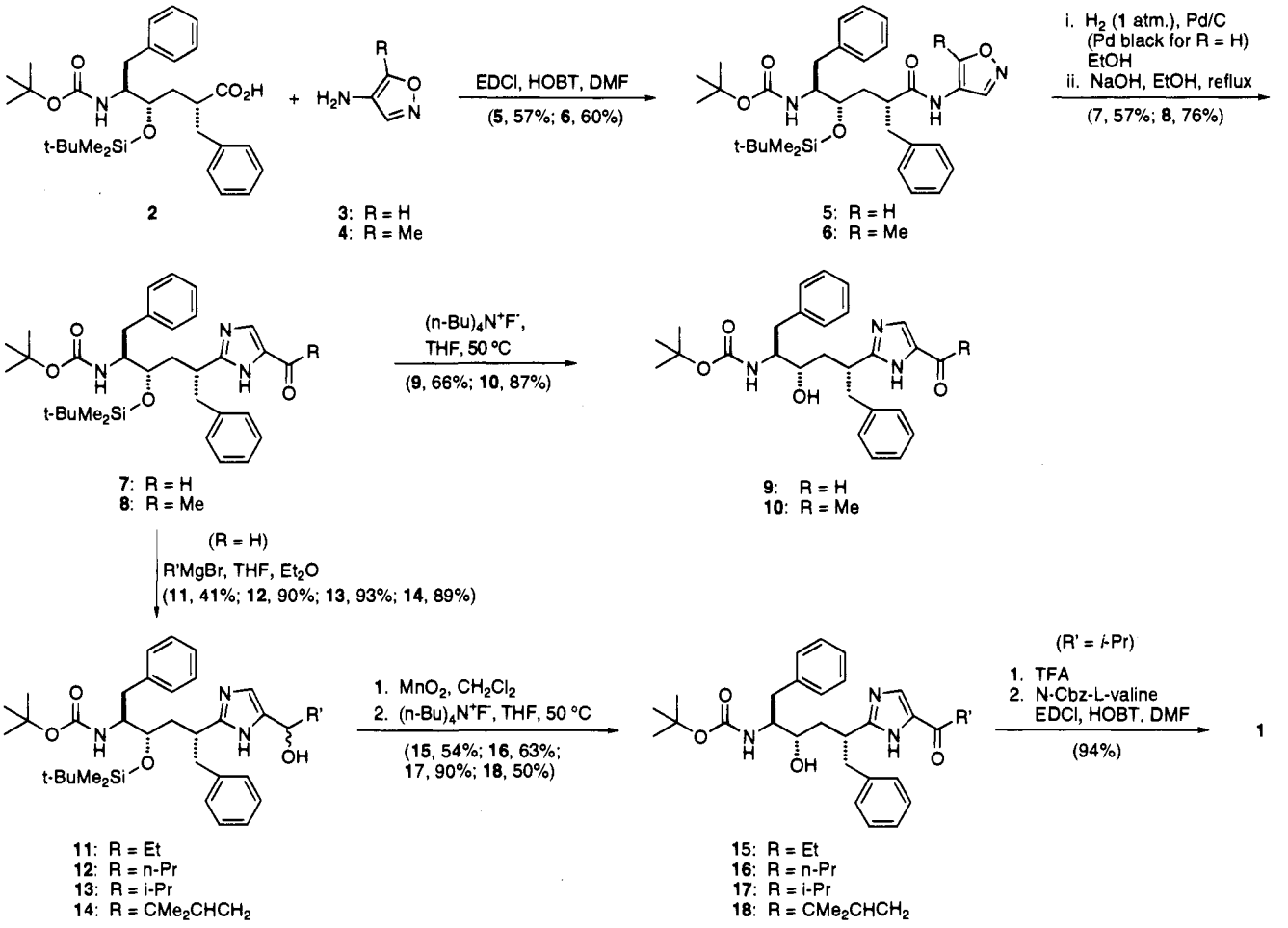

Scheme 2

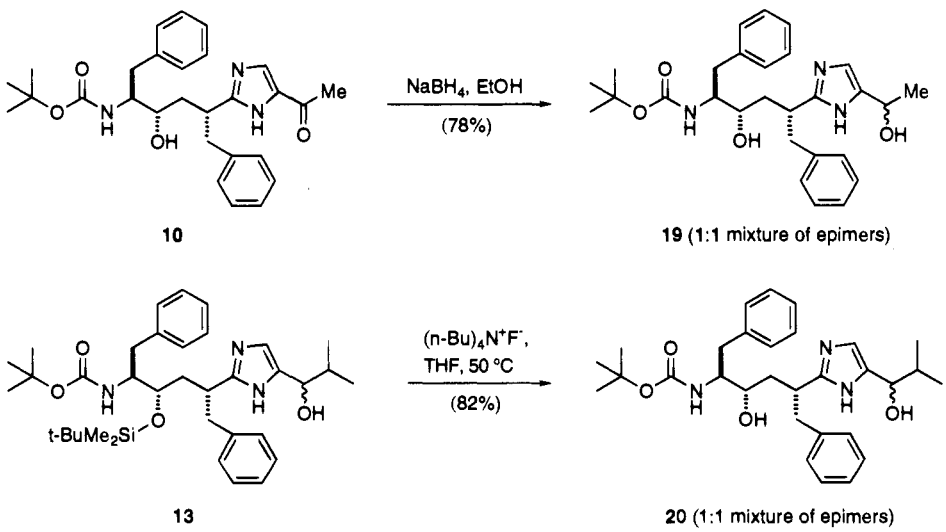

structure with only one orientation of the inhibitor was compared to refinement with both orientations, a slight improvement of the *R*-factor and a better fit to the electron density were evident. The electron density of the inhibitor is almost symmetric, and both orientations of the inhibitor fit the electron density well.

Protein Structure. The structure of the protein is nearly identical to that of previously reported HIV-1 protease/inhibitor complexes. Superposition of backbone atoms from our protease dimer structure with those from the structures containing inhibitors MVT-101,[29] A74704,[18] Acetylpepstatin,[36] L700,417,[19] and SB 204144[20] gives rms deviations of 0.6, 0.4, 0.7, 0.6, and 0.4 Å, respectively. Superposition of the backbone atoms of the two protease subunits of this SB 206343-containing structure gives an rms deviation of 0.4 Å, while superposition of all atoms, including side chain atoms, gives an rms deviation of 1.1 Å, indicating conservation of the symmetry of the homodimer.

Binding of the Inhibitor. The inhibitor is present in the active site of the enzyme in an extended conformation with every heteroatom of the inhibitor hydrogen-

Table 2. Inhibition of HIV-1 Protease[a]

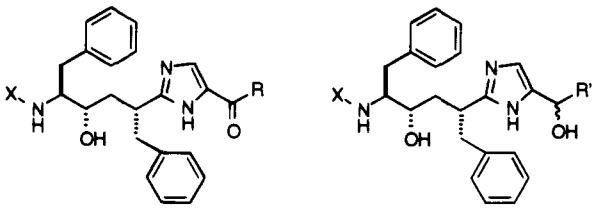

compd	X	R (or R')	formula[b]	apparent K_i (nM)
1	Cbz-Val	*i*-Pr	$C_{38}H_{46}N_4O_5 \cdot 0.25H_2O$	0.6 ± 0.1[c]
9	Boc	H	$C_{27}H_{33}N_3O_4 \cdot 0.5H_2O$	3500 ± 240[d]
10	Boc	Me	$C_{28}H_{35}N_3O_4 \cdot 0.75H_2O$	370 ± 46
15	Boc	Et	$C_{29}H_{37}N_3O_4 \cdot 0.75H_2O$	92 ± 8
16	Boc	*n*-Pr	$C_{30}H_{39}N_3O_4 \cdot 0.5H_2O$	150 ± 20
17	Boc	*i*-Pr	$C_{30}H_{39}N_3O_4 \cdot 0.5H_2O$	83 ± 11
18	Boc	CMe_2CHCH_2	$C_{32}H_{41}N_3O_4 \cdot 0.5H_2O$	270 ± 12
19	Boc	Me (R')	$C_{28}H_{37}N_3O_4 \cdot 0.5H_2O$	13 300 ± 1320
20	Boc	*i*-Pr (R')	$C_{30}H_{41}N_3O_4 \cdot 1.15H_2O$	2700 ± 150
Boc-Pheψ(CHOHCH$_2$)PheGlyNH$_2$				120 ± 7[e]
Cbz-AlaPheψ(CHOHCH$_2$)PheValNH$_2$				0.7 ± 0.1[f]

[a] Assays were conducted at 37 °C, pH 6.0 (0.2 M NaCl), as previously described.[43,44] [b] Satisfactory analyses (C, H, and N; ±0.4% of theoretical values) were obtained for all compounds. [c] Determined from plots of remaining enzymatic initial rate as a function of inhibitor concentration at several fixed enzyme concentrations as previously described (Dreyer et al., 1992). [d] Determined by Dixon analysis. [e] Dreyer, G. B. Unpublished results. [f] Reference 33.

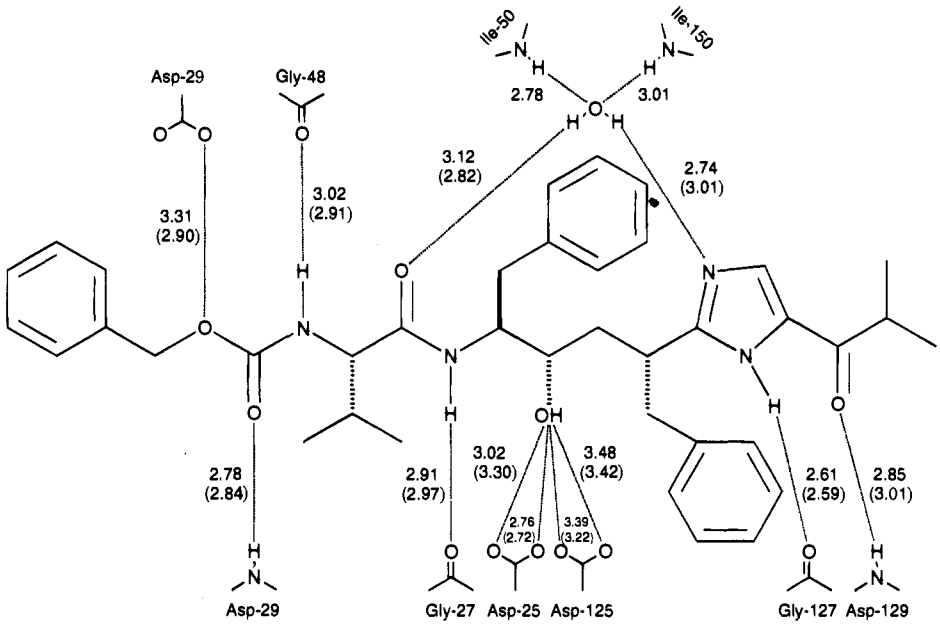

Figure 2. Schematic representation of SB 206343 bound in the active site of HIV-1 protease. Potential hydrogen bond interactions between the inhibitor and the active site amino acid residues of the protein are indicated by dotted lines. Distances between non-hydrogen atoms are given in angstroms for both orientations of the inhibitor, with the distances for the second orientation in parentheses.

bonded to the protein either directly or indirectly through a water molecule. These interactions are depicted schematically in Figure 2, with distances between non-hydrogen atoms in angstroms for both orientations of the inhibitor (second orientation shown in parentheses), and three-dimensionally in Figure 3. The structural water molecule is tetrahedrally bound to the flaps via hydrogen bonds to the backbone amide nitrogens of Ile-50 and Ile-150 and to the inhibitor via hydrogen bonds to N-3 of the imidazole ring and the carbonyl oxygen of the P_2 valine residue. Notably, the water molecule is bound symmetrically between the imidazole ring and the valine carbonyl, demonstrating the effectiveness and fidelity of the 4(5)-acylimidazole ring as an isosteric amide bond replacement in a hydroxyethylene-based HIV-1 protease inhibitor. Also noteworthy are the hydrogen bonds connecting N-1 of the imidazole and the imidazole acyl carbonyl oxygen with the Gly-127 carbonyl and Asp-129 backbone nitrogen, respectively, thus exemplifying the peptidomimetic nature of the 4(5)-acylimidazole isostere. These hydrogen-bonding interactions are identical to those observed for the P_1'–P_2' amide groups found in virtually all HIV-1 protease inhibitors. The contribution of the alkyl portion of the imidazole acyl substituent toward binding of the inhibitor can be straightforwardly inferred from the crystallographic data. One of the methyl groups of the acyl substituent in SB 206343 is bound in the hydrophobic S_2' subsite of the enzyme, while the other is oriented along the peptide backbone.

Comparison with the MVT-101 Structure. Figure 4 shows the superposition of SB 206343 and MVT-101

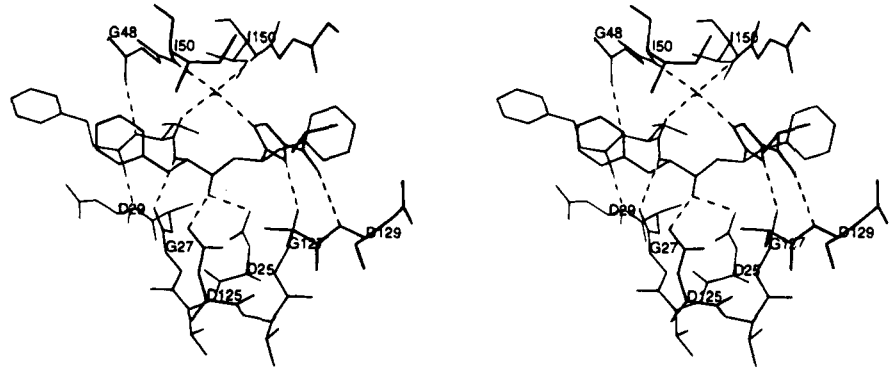

Figure 3. Stereoview of SB 206343 bound in the active site of HIV-1 protease.

Figure 4. Stereoview of the overlay of the active site conformations of SB 206343 (one orientation, solid lines) and MVT-101 (dashed lines).

in the active site of HIV-1 protease, achieved by superimposing all backbone atoms of the two proteins. The superpositions show a high degree of overlap between side chain groups as well as backbone atoms, with the benzyl portion of the Cbz group occupying the S_3 subsite (occupied by a Thr side chain in MVT-101) and one of the methyl groups of the imidazole acyl substituent occupying the S_2' subsite (occupied by a Gln side chain in MVT-101). All of the polar interactions are also conserved for the two structures.

Conclusions

Using a model derived from the structure of the MVT-101/HIV-1 protease complex, we have accomplished the rational design and synthesis of potent, hydroxyethylene-based HIV-1 protease inhibitors that contain a 4(5)-acylimidazole as a P_1'—P_2' amide bond isostere. SAR data and X-ray crystallographic studies of HIV-1 protease complexed to one such inhibitor, SB 206343, have revealed that this particular heterocyclic isostere is an excellent peptidomimetic, participating in all polar and hydrophobic interactions that are commonly observed between enzymes and peptidic inhibitors.

Experimental Section

Unless otherwise noted, materials were obtained from commercial suppliers and used without further purification. THF was distilled from sodium/benzophenone ketyl. DMF was anhydrous grade (Aldrich). Grignard reagents were prepared according to a published procedure.[37] All reactions involving organometallic reagents were conducted under an atmosphere of dry argon in oven-dried glassware. Electrospray ionization mass spectra (MS-(ESI)) were obtained with a Sciex API-III triple quadrupole mass spectrometer. ^{1}H NMR spectra were obtained at 250 or 400 MHz. When ^{1}H NMR spectra were obtained on mixtures of stereoisomers or tautomers, some of the resonances overlapped. Therefore, the correct number of resonances may not be listed. All ^{1}H NMR spectra were obtained as solutions in $CDCl_3$. All extracts were dried over anhydrous magnesium sulfate, and solvents were removed with a Buchi rotary evaporator at aspirator pressure. Flash chromatography using Kieselgel 60 silica gel was performed as previously reported.[38]

(2*R*,4*S*,5*S*)-2-Benzyl-5-[(*tert*-butoxycarbonyl)amino]-4-(*tert*-butyldimethylsiloxy)-*N*-(isoxazol-4-yl)-6-phenylhexanamide (5). To a mixture containing (2*R*,4*S*,5*S*)-2-benzyl-5-[(*tert*-butoxycarbonyl)amino]-4-(*tert*-butyldimethylsiloxy)-6-phenylhexanoic acid (**2**) (8.34 g, 15.8 mmol), 1-hydroxybenzotriazole (427 mg, 3.2 mmol), and 1-[3-(dimethylamino)propyl]-3-ethylcarbodiimide hydrochloride (3.33 g, 17.4 mmol) in 80 mL of DMF was added 4-aminoisoxazole (**3**) (1.46 g, 17.4 mmol). The resulting solution was allowed to stir at room temperature for 24 h and then was poured into water and extracted with ethyl acetate. The extract was washed successively with 0.1 N HCl, saturated aqueous $NaHCO_3$, and saturated brine and then dried, filtered, and concentrated. The residue was purified by flash chromatography, eluting with 1:5 ethyl acetate/hexanes to give 5.35 g (57%) of **5** as a white solid: ^{1}H NMR δ 8.91 (s, 1) 8.34 (br s, 1), 8.24 (s, 1), 7.37–7.18 (m, 8), 7.02 (d, 2), 4.75 (d, 1), 4.11–4.01 (m, 1), 3.64 (dd, 1), 3.16 (dd, 1), 2.81–2.50 (m, 4), 1.85–1.65 (m, 4), 1.32 (s, 9), 0.93 (s, 9), 0.10 (s, 3), 0.09 (s, 3).

Compound **6** was prepared in this manner from 5-methyl-4-aminoisoxazole (**4**).

2-[(1*R*,3*S*,4*S*)-1-Benzyl-4-[(*tert*-butoxycarbonyl)amino]-3-(*tert*-butyldimethylsiloxy)-5-phenylpentyl]-4(5)-formylimidazole (7). A mixture containing compound **5** (1.21 g, 2.04 mmol) and palladium black (0.6 g) in 20 mL of ethanol was stirred under a hydrogen atmosphere for 2 h. The mixture was purged with argon, and an additional 0.6 g of palladium black was added. Stirring under a hydrogen atmosphere was continued for an additional 21 h. The mixture was purged with argon for 20 min and filtered through a bed of Celite, and the filtrate was concentrated. The residue was dissolved in 20 mL of ethanol, and 1 M NaOH in ethanol (2.65 mL, 2.65 mmol) was added. The resulting mixture was heated at reflux for 3 h and then partitioned between ethyl acetate and aqueous NH_4Cl. The extract was washed with saturated brine, dried, filtered, and concentrated. The oily residue was purified by flash chromatography, eluting with 1:1 ethyl acetate/hexanes to afford 675.6 mg (57%) of **7** as a yellow solid: ^{1}H NMR (mixture of tautomers) δ 10.71 (br s, 1), 10.47 (br s, 1), 9.86 (s, 1), 9.56 (s, 1), 7.66 (s, 1), 7.51 (d, 1), 7.36–6.99 (m, 20), 4.77 (d, 1), 4.70 (d, 1), 4.14–4.04 (m, 2), 3.60 (t, 1), 3.49–3.41 (m, 1), 3.35–3.08 (m, 2), 2.90–2.62 (m, 6), 1.83–1.75 (m, 4), 1.36 (s, 9), 1.35 (s, 9), 0.91 (s, 9), 0.89 (s, 9), 0.05–0.02 (m, 12).

2-[(1*R*,3*S*,4*S*)-1-Benzyl-4-[(*tert*-butoxycarbonyl)amino]-3-(*tert*-butyldimethylsiloxy)-5-phenylpentyl]-4(5)-acetylimidazole (8). A mixture containing compound **6** (185.8 mg, 0.31 mmol) and 10% palladium on activated carbon (93 mg) in 3 mL of ethanol was stirred under a hydrogen atmosphere for 5 h. The mixture was purged with argon for 20 min and filtered through a bed of Celite, and the filtrate was concentrated. The residue was dissolved in 3 mL of ethanol, and 1M NaOH in ethanol (0.4 mL, 0.4 mmol) was added. The resulting

mixture was heated at reflux overnight and then partitioned between ethyl acetate and aqueous NH_4Cl. The extract was washed with saturated brine, dried, filtered, and concentrated. The oily residue was purified by flash chromatography, eluting with 1:2 ethyl acetate/hexanes to afford 136.8 mg (76%) of **8** as a yellow solid: ^1H NMR (mixture of tautomers) δ 7.58 (s, 1), 7.47 (d, 1), 7.34–7.07 (m, 18), 7.00 (d, 2), 4.78 (d, 1), 4.67 (d, 1), 4.08 (m, 2), 3.65–3.59 (m, 1), 3.49–3.40 (m, 2), 3.30–3.22 (m, 2), 3.06 (m, 1), 2.86–2.78 (m, 2), 2.71–2.64 (m, 4), 2.53 (s, 3), 2.36 (s, 3), 1.84–1.61 (m, 4), 1.36 (s, 9), 1.35 (s, 9), 0.91 (s, 9), 0.89 (s, 9), 0.05 (s, 6), 0.00 (s, 6).

2-[(1*R*,3*S*,4*S*)-Benzyl-4-[(*tert*-butoxycarbonyl)amino]-3-hydroxy-5-phenylpentyl]-4(5)-acetylimidazole (10). A solution containing compound **8** (61.6 mg, 0.1 mmol) in 1.25 mL of 1 M tetra-*n*-butylammonium fluoride in THF was heated at 50 °C for 5 h. The solution was then poured into ethyl acetate, washed successively with water (2x) and saturated brine, dried, filtered, and concentrated. The residue was purified by flash chromatography, eluting with 2:1 ethyl acetate/hexanes to give 41.7 mg (84%) of **10** as a white solid: ^1H NMR δ 7.60 (br s, 1), 7.24–7.13 (m, 8), 6.92 (m, 2), 4.92 (m, 1), 3.61 (d, 2), 3.37 (m, 1), 3.10–3.02 (m, 1), 2.91–2.84 (m, 3), 2.42 (s, 3), 1.98–1.81 (m, 2), 1.36 (s, 9); MS-(ESI) *m/z* 478.2 $(M + H)^+$. Anal. ($C_{28}H_{35}N_3O_4 \cdot 0.75H_2O$) C, H, N.

Compound **9** was prepared in this manner from compound **7**.

2-[(1*R*,3*S*,4*S*)-1-Benzyl-4[(*tert*-butoxycarbonyl)amino]-3-(*tert*-butyldimethylsiloxy)-5-phenylpentyl]-4(5)-(1-hydroxy-2-methylpropyl)imidazole (13). To a solution of compound **7** (500 mg, 0.98 mmol) in 2 mL of 1:1 Et_2O/THF was added dropwise a 3 M solution of isopropylmagnesium bromide in Et_2O (1.73 mL, 5.2 mmol). After the mixture had stirred for 15 min, the reaction was quenched by the addition of aqueous NH_4Cl and the mixture was extracted with ethyl acetate. The extract was washed with saturated brine, dried, filtered, and concentrated. The residue was purified by flash chromatography, eluting with 1:1 ethyl acetate/hexanes to give 502.7 mg (93%) of **13** as a pale yellow solid: ^1H NMR (mixture of diastereomers) δ 7.28–6.58 (m, 11), 4.80–4.54 (m, 1), 4.29 (m, 1), 4.02 (m, 1), 3.64–3.55 (m, 2), 3.25 (m, 1), 3.02 (m, 1), 2.72–2.54 (m, 3), 1.77 (m, 2), 1.35–1.23 (m, 9), 1.00–0.81 (m, 15), 0.10–0.00 (m, 6).

Compounds **11**, **12**, and **14** were prepared in this manner.

2-[(1*R*,3*S*,4*S*)-1-Benzyl-4-[(*tert*-butoxycarbonyl)amino]-3-(*tert*-butyldimethylsiloxy)-5-phenylpentyl]-4(5)-(2-methylpropionyl)imidazole (17-OTBS). To a solution of compound **13** (77.6 mg. 0.12 mmol) in 1 mL of CH_2Cl_2 was added MnO_2 (775 mg), and the resulting suspension was allowed to stir at room temperature. The reaction mixture was filtered through a bed of Celite, and the filtrate was concentrated. The residue was purified by flash chromatography, eluting with 1:2 ethyl acetate/hexanes to give 70 mg (90%) of **17-OTBS** as a white solid: ^1H NMR (mixture of tautomers) δ7.60 (s, 1), 7.48 (d, 1), 7.34–6.98 (m, 20), 4.77–4.66 (m, 2), 4.10–4.03 (m, 2), 3.64–3.59 (m, 3), 3.23–3.04 (m, 5), 2.87–2.60 (m, 6), 1.84–1.75 (m, 4), 1.36 (s, 9), 1.33 (s, 9), 1.24–1.14 (m, 12), 0.91 (s, 18), 0.05–0.00 (m, 12).

Compounds **15-OTBS**, **16-OTBS**, and **18-OTBS** were prepared in this manner.

2-[(1*R*),3*S*,4*S*)-1-Benzyl-4-[(*tert*-butoxycarbonyl)amino]-3-hydroxy-5-phenylpentyl)]-4(5)-(2-methylpropionyl)-imidazole (17). A solution containing compound **17-OTBS** (2.82 g, 4.55 mmol) in 50 mL of 1 M tetra-*n*-butylammonium fluoride in THF was heated at 50 °C for 5 h. The solution was then poured into ethyl acetate, washed successively with water (2x) and saturated brine, dried, filtered, and concentrated. The residue was purified by flash chromatography, eluting with 2:1 ethyl acetate/hexanes to give 2.3 g (100%) of **17** as a white solid: ^1H NMR δ 7.62 (s, 1), 7.34–7.04 (m, 8), 6.91–6.88 (m, 2), 5.11–4.91 (m, 2), 3.61–3.52 (m, 2), 3.43–3.40 (m, 1), 3.19 (septet, 1), 3.10–3.02 (m, 1), 3.07–2.83 (m, 3), 1.98–1.94 (m, 1), 1.81–1.75 (m, 1), 1.35 (s, 9), 1.21 (d, 3), 1.19 (d, 3); MS-(ESI) *m/z* 506.2 $(M + H)^+$. Anal. ($C_{30}H_{39}N_3O_4 \cdot 0.5H_2O$) C, H. N.

Compounds **15**, **16**, and **18** were prepared in this manner.

2-[(1*R*,3*S*,4*S*)-1-Benzyl-4-[[*N*-(benzyloxycarbonyl)-*L*-valyl]amino]-3-hydroxy-5-phenylpentyl]-4(5)-(2-methylpropionyl)imidazole (1). A solution containing compound **17** (200.4 mg, 0.40 mmol) in 1 mL of TFA was stirred at room temperature for 5 min and then was concentrated under reduced pressure. The residue was partitioned between ethyl acetate and 10% aqueous NaOH, and the aqueous phase was extracted with ethyl acetate (2x). The combined extracts were dried, filtered, and concentrated to give 160.5 mg (100%) of 2-[(1*R*,3*S*,4*S*)-4-amino-1-benzyl-3-hydroxy-5-phenylpentyl]-4(5)-(2-methylpropionyl)imidazole as a white solid: ^1H NMR δ 7.61 (s, 1), 7.26–7.05 (m, 10), 3.45 (m, 1), 3.18 (m, 3), 2.89–2.82 (m, 3), 2.44 (m, 1), 2.06 (m, 1), 1.83 (m, 1), 1.16 (d, 6). This material was used in the next step without further purification.

A mixture containing 2-[(1*R*,3*S*,4*S*)-4-amino-1-benzyl-3-hydroxy-5-phenylpentyl]-4(5)-(2-methylpropionyl)imidazole (3.7 mg. 9 μmol), *N*-Cbz-L-valine (2.3 mg, 9 μmol), 1-hydroxybenzotriazole (0.2 mg, 2 μmol), and 1-[3-(dimethylamino)propyl]-3-ethylcarbodiimide hydrochloride (1.9 mg, 10 μmol) in 0.2 mL of DMF was allowed to stir at room temperature overnight. The reaction mixture was poured into ethyl acetate and washed successively with water, 0.1 N HCl, saturated aqueous $NaHCO_3$, and saturated brine and then dried, filtered, and concentrated. The residue was purified by flash chromatography, eluting with 4% MeOH in CH_2Cl_2 to afford 5.5 mg (94%) of **1** as a white solid: ^1H NMR δ 7.55 (s, 1), 7.31–6.68 (m, 16), 5.44 (d, 1), 5.18–5.04 (m, 2), 4.01–3.92 (m, 2), 3.60 (d, 1), 3.42 (m, 1), 3.18–3.02 (m, 2), 2.85 (m, 3), 2.03–1.74 (m, 3), 1.18 (d, 6), 0.81 (d, 3), 0.74 (d, 3); MS-(ESI) *m/z* 639.4 $(M + H)^+$. Anal. ($C_{38}H_{46}N_4O_5 \cdot 0.25H_2O$) C, H, N.

2-[(1*R*,3*S*,4*S*)-1-Benzyl-4-[(*tert*-butoxycarbonyl)amino]-3-hydroxy-5-phenylpentyl]-4(5)-(1-hydroxyethyl)imidazole (19). To a solution of compound **10** (20.8 mg, 0.044 mmol) in 0.5 mL of EtOH was added excess $NaBH_4$. After the mixture had stirred for 15 min, the reaction was quenched by the addition of aqueous NH_4Cl and the mixture was extracted with ethyl acetate. The extract was washed with saturated brine, dried, filtered, and concentrated. The residue was purified by flash chromatography, eluting with ethyl acetate to afford 16.3 mg (78%) of **19** as a white solid: ^1H NMR (mixture of diastereomers) δ 7.31–7.17 (m, 16), 6.90–6.88 (m, 4), 6.66 (s, 2), 5.01 (d, 2), 4.84 (m, 2H), 3.62 (m, 4), 3.24 (m, 2), 3.01–2.86 (m, 8), 1.97 (m, 2), 1.75 (m, 2), 1.51 (d, 3), 1.48 (d, 3), 1.36 (s, 18); MS-(ESI) *m/z* 480.4 $(M + H)^+$. Anal. ($C_{28}H_{37}N_3O_4 \cdot 0.5H_2O$) C, H, N.

2-[(1*R*,3*S*,4*S*)-1-Benzyl-4-[(*tert*-butoxycarbonyl)amino]-3-hydroxy-5-phenylpentyl]-4(5)-(1-hydroxy-2-methylpropyl)imidazole (20). A solution containing compound **13** (10.0 mg, 0.016 mmol) in 0.3 mL of 1 M tetra-*n*-butylammonium fluoride in THF was heated at 50 °C for 2 h. The solution was then poured into ethyl acetate, washed successively with water (2x) and saturated brine, dried, filtered, and concentrated. The residue was purified by flash chromatography, eluting with 1:3 ethyl acetate/hexanes and then with ethyl acetate to afford 6.7 mg (82%) of compound **20** as a white solid: ^1H NMR δ 7.26–7.15 (m, 8), 6.90 (m, 2), 6.63 (m, 1), 5.04 (m, 1), 4.34 (m, 1), 3.61 (m, 2), 3.27 (m, 1), 2.85 (m, 4), 1.96 (m, 2), 1.75 (m, 2), 1.35 (s, 9), 0.99–0.80 (m, 6); MS-(ESI) *m/z* 508.2 $(M + H)^+$. Anal. ($C_{30}H_{41}N_3O_4 \cdot H_2O$) C, H, N.

Enzyme Preparation. Recombinant HIV-1 protease, derived from the BH10 clone of HIV-1,[39] was obtained by expression in *Escherichia coli*[40] and purified to apparent homogeneity as previously described.[41] The purified protease was stored in 50 mM sodium acetate (pH 5.0), 0.35 M NaCl, 1 mM EDTA, 1 mM DTT, and 20–40% glycerol at −40 °C, and its concentration was determined by the chromatographic method of Strickler.[42] The protease/SB 206343 inhibitor complex was prepared by adding a 10 mM aqueous solution of the inhibitor to a 0.2 mg/mL protein solution. The complex was then concentrated by ultrafiltration to a final protein concentration of approximately 5 mg/mL, at room temperature.

Enzyme Inhibition Assays. Peptidolysis reactions were conducted at 37 °C in a buffer composed of 50 mM 2-(*N*-morpholino)ethanesulfonic acid (pH 6.0, 1 mM EDTA, 200 mM NaCl, 1 mM dithiothreitol, 0.1% Triton X-100, and 10% v/v

DMSO) in reaction mixtures containing 1–10 mM concentrations of the substrate Ac-RASQNYPVV-NH_2, variable concentrations of the inhibitor, and 20 nM HIV-1 protease. HPLC quantification of reaction products and determination of inhibition constants (Dixon analysis) were performed as previously described.[43,44] For compounds which were inhibitory at concentrations equivalent to those of the enzyme, apparent inhibition constants were obtained from plots of remaining initial rate vs inhibitor concentration at several fixed enzyme concentrations, as described.[33]

Crystallography. The complex of SB 206343 with HIV-1 protease was crystallized as described previously.[29] Typically, cocrystals were grown by the method of vapor diffusion in hanging drops[45] by using 18–26% saturated ammonium sulfate buffered at pH 5.0 with 200 mM acetate as the precipitant. The symmetry of the diffraction was consistent with that of the hexagonal space group $P6_122$ or $P6_1$ with strong noncrystallographic 22 symmetry resulting from the 2-fold symmetry of the protein. We chose the latter space group to be consistent with the previously reported crystal structures of HIV-1 protease/inhibitor complexes.[18,2033,35] The unit cell dimensions were $a = b = 63.0$ Å and $c = 83.3$ Å, with the asymmetric unit containing one complete copy of the complex (a protein dimer plus an inhibitor).

X-ray diffraction data were measured from a single crystal using a Siemens two-dimensional position-sensitive detector. The detector was mounted on a Siemens rotating anode X-ray generator operated at 50 kV and 96 mA, equipped with a 300 μm focusing cup, and producing graphite-monochromated CuKα radiation. Diffraction images were recorded, reduced and visualized using FRAMBO, XENGEN,[46] and XPREP computer programs, respectively. Approximately 39 160 reflections were measured in 2 days to give 8866 unique reflections to 2.24 Å resolution, representing 98% of the data.

Crystallographic refinement was carried out using the restrained least-squares program PROLSQ.[47] Minor modifications to the export version[48] of this program allowed for its use on a Silicon Graphics IRIS 4D/380 and for the ability to run multiple cycles of refinement without manual intervention. The starting model used in refinement consisted of the protein portion of the 2.8 Å structure of A74704 complexed to HIV-1 protease.[18] A few cycles of rigid body least-squares refinement using data to 3.0 Å resolution for reflections greater than $3\sigma(F_o)$ were carried out to obtain the optimal position and orientation of the starting model. This was followed by iterative cycles of refinement and model building. Fourier maps with coefficients $|F_o| - |F_c|$ and $2|F_o| - |F_c|$ were computed and displayed on an Evans and Sutherland PS300 graphics system using FRODO.[49] Maps calculated using refined phases, obtained from data greater than $2.0\sigma(F_o)$ in the resolution range of 8.0–2.5 Å, showed clear electron density for the inhibitor. A model of SB 206343 was positioned in the electron density, and the complex was further refined. Special bond and angle distances were incorporated in the program PROTIN[47] to account for the geometry of the inhibitor. To account for the 2-fold disorder observed in the $P6_1$ crystal lattice, resulting from the symmetric nature of the protein,[33–35] a second inhibitor molecule was introduced and the protein and the two inhibitors (each at half-occupancy) were simultaneously refined. This was followed by refinement using XPLOR[50] and the positioning of water molecules. Statistics from the crystallographic refinement are detailed in Table 1. The refined set of atomic coordinates has been deposited in the Protein Data Bank.[51]

Acknowledgment. We thank Walter Holl for pK_a measurements of compounds **10** and **17** and Edith Reich for performing the elemental analyses.

References

(1) Varmus, H.; Swanstrom, R. In *RNA Tumor Viruses: Molecular Biology of Tumor Viruses*; Weiss, R., Teich, N., Varmus, H., Coffin, J., Eds.; Cold Spring Harbor Laboratory: Cold Spring Harbor, NY, 1985; Vol. 1, pp 369–512.
(2) Gallo, R. C.; Montagnier, L. AIDS in 1988. *Sci. Am.* **1988**, *259*, 40–48.
(3) Kramer, R. A.; Schaber, M. D.; Skalka, A. M.; Ganguly, K.; Wong-Staal, F.; Reddy, E. P. HTLV-III gag Protein Is Processed in Yeast by the Virus pol-Protease. *Science* **1986**, *231*, 1580–1585.
(4) Kohl, N. E.; Emini, E. A.; Schleif, W. A.; Davis, L. J.; Heimbach, J. C.; Dixon, R. A.; Scolnick, E. M.; Sigal, I. S. Active Human Immunodeficiency Virus Protease is Required for Viral Infectivity. *Proc. Natl. Acad. Sci. U.S.A.* **1988**, *85*, 4686–4690.
(5) Toh, H.; Ono, M.; Saigo, K.; Miyata, T. Retroviral Protease-Like Sequence in the Yeast Transposon Ty1. *Nature* **1985**, *315*, 691–692.
(6) Power, M. D.; Marx, P. A.; Bryant, M. L.; Garnder, M. B.; Barr, P. J.; Luciw, P. A. Nucleotide Sequence of SRV-1, a Type-D Simian Acquired Immune Deficiency Syndrome Retrovirus. *Science* **1986**, *231*, 1567–1572.
(7) Pearl, L. H.; Taylor, W. R. A Structural Model for the Retroviral Proteases. *Nature* **1987**, *329*, 351–354.
(8) Lapatto, R.; Blundell, T.; Hemmings, A.; Overington, J.; Wilderspin, A.; Wood, S.; Merson, J. R.; Whittle, P. J.; Danley, D. E.; Geoghegan, K. F.; Hawrylik, S. J.; Lee, S. E.; Scheld, K. G.; Hobart, P. M. X-ray Analysis of HIV-1 Proteinase at 2.7 Å Resolution Confirms Structural Homology Among Retroviral Enzymes. *Nature* **1989**, *342*, 299–302.
(9) Navia, M. A.; Fitzgerald, P. M.; McKeever, B. M.; Leu, C. T.; Heimbach, J. C.; Herber, W. K.; Sigal, I. S.; Darke, P. L.; Springer, J. P. Three-Dimensional Structure of Aspartyl Protease from Human Immunodeficiency Virus HIV-1. *Nature* **1989**, *337*, 615–620.
(10) Wlodawer, A.; Miller, M.; Jaskolski, M.; Sathyanarayana, B. K.; Baldwin, E.; Weber, I. T.; Selk, L. M.; Clawson, L.; Schneider, J.; Kent, S. B. H. Conserved Folding in Retroviral Proteases: Crystal Structure of a Synthetic HIV-1 Protease. *Science* **1989**, *245*, 616–621.
(11) For a review, see Fitzgerald, P. M. D. HIV Protease-Ligand Complexes. *Curr. Opin. Struct. Biol.* **1993**, *3*, 868–874.
(12) Mulichak, A. M.; Hui, J. O.; Tomasselli, A. G.; Heinrikson, R. L.; Curry, K. A.; Tomich, C.-S.; Thaisrivongs, S.; Sawyer, T. K.; Watenpaugh, K. D. The Crystallographic Structure of the Protease from Human Immunodeficiency Virus Type 2 with Two Synthetic Peptidic Transition State Analog Inhibitors. *J. Biol. Chem.* **1993**, *268*, 13103–13109.
(13) Tong, L.; Pav, S.; Pargellis, C.; Dô, F.; Lamarre, D.; Anderson, P. C. Crystal Structure of Human Immunodeficiency Virus (HIV) Type 2 Protease in Complex with a Reduced Amide Inhibitor and Comparison with HIV-1 Protease Structures. *Proc. Natl. Acad. Sci. U.S.A.* **1993**, *90*, 8387–8391.
(14) Rose, R. B.; Rosé, J. R.; Salto, R.; Craik, C. S.; Stroud, R. M. Structure of the Protease from Simian Immunodeficiency Virus: Complex with an Irreversible Nonpeptide Inhibitor. *Biochemistry* **1993**, *32*, 12498–12507.
(15) Zhao, B.; Winborne, E.; Minnich, M. D.; Culp, J. S.; Debouck, C.; Abdel-Meguid, S. S. Three-Dimensional Structure of a Simian Immunodeficiency Virus Protease/Inhibitor Complex. Implications for the Design of Human Immunodeficiency Virus Type 1 and 2 Protease Inhibitors. *Biochemistry* **1993**, *32*, 13054–13060.
(16) Lam, P. Y. S.; Jadhav, P. K.; Eyermann, C. J.; Hodge, C. N.; Ru, Y.; Bacheler, L. T.; Meek, J. L; Otto, M. J.; Rayner, M. M.; Wong, Y. N.; Chang, C.-H.; Weber, P. C.; Jackson, D. A.; Sharpe, T. R.; Erickson-Viitanen, S. *Rational* Design of Potent, Bioavailable, Nonpeptide Cyclic Ureas as HIV Protease Inhibitors. *Science* **1994**, *263*, 380–384.
(17) Greenlee, W. J. Renin Inhibitors. *Med. Res. Rev.* **1990**, *10*, 173–236.
(18) Abdel-Meguid, S. S. Inhibitors of Aspartyl Proteinases. *Med. Res. Rev.* **1993**, *13*, 731–778.
(19) Erickson, J.; Neidhart, D. J.; VanDrie, J.; Kempf, D. J.; Wang, X. C.; Norbeck, D. W.; Plattner, J. J.; Rittenhouse, J. W.; Turon, M.; Wideburg, N.; Kohlbrenner, W. E.; Simmer, R.; Helfrich, R.; Paul, D.; Knigge, M. Design, Activity, and 2.8 Å Crystal Structure of a C_2 Symmetric Inhibitor Complexed to HIV-1 Protease. *Science* **1990**, *249*, 527–533.
(20) Bone, R.; Vacca, J. P.; Anderson, P. S.; Holloway, M. K. X-ray Crystal Structure of the HIV Protease Complex with L-700,417, an Inhibitor with Pseudo C_2 Symmetry. *J. Am. Chem. Soc.* **1991**, *113*, 9382–9384.
(21) Abdel-Meguid, S. S.; Zhao, B.; Murthy, K. H. M.; Winborne, E.; Choi, J.-K.; DesJarlais, R. L.; Minnich, M. D.; Culp, J. S.; Debouck, C.; Tomaszek, T. A., Jr.; Meek, T. D.; Dreyer, G. B. Inhibition of Human Immunodeficiency Virus-1 Protease by a C_2-Symmetric Phosphinate. Synthesis and Crystallographic Analysis. *Biochemistry* **1993**, *32*, 7972–7980.
(22) McQuade, T. J.; Tomasselli, A. G.; Liu, L.; Karacostas, V.; Moss, B.; Sawyer, T. K.; Heinrikson, R. L.; Tarpley, W. G. A Synthetic HIV-1 Protease Inhibitor with Antiviral Activity Arrests HIV-Like Particle Maturation. *Science* **1990**, *247*, 454–456.
(23) Meek, T. D.; Lambert, D. M.; Dreyer, G. B.; Carr, T. J.; Tomaszek, T. A.; Moore, M. L.; Strickler, J. E.; Debouck, C.; Hyland, L. J.; Matthews, T. J.; Metcalf, B. W.; Petteway, S. R. Inhibition of HIV-1 Protease in Infected T-lymphocytes by Synthetic Peptide Analogues. *Nature* **1990**, *343*, 90–92.

(24) Roberts, N. A.; Martin, J. A.; Kinchington, D.; Broadhurst, A. V.; Craig, J. C.; Duncan, I. B.; Galpin, S. A.; Handa, B. K.; Kay, J.; Kröhn, A.; Lambert, R. W.; Merrett, J. H.; Mills, J. S.; Parkes, K. E. B.; Redshaw, S.; Ritchie, A. J.; Taylor, D. L.; Thomas, G. J.; Machin, P. J. Rational Design of Peptide-Based HIV Proteinase Inhibitors. *Science* **1990**, *248*, 358–361.

(25) Thompson, W. J.; Fitzgerald, P. M. D.; Holloway, M. K.; Emini, E. A.; Darke, P. L.; McKeever, B. M.; Schleif, W. A.; Quintero, J. C.; Zugay, J. A.; Tucker, T. J.; Schwering, J. E.; Homnick, C. F.; Nunberg, J.; Springer, J. P.; Huff, J. R. Synthesis and Antiviral Activity of a Series of HIV-1 Protease Inhibitors with Functionality Tethered to the P_1 or P_1' Phenyl Substituents: X-ray Crystal Structure Assisted Design. *J. Med. Chem.* **1992**, *35*, 1685–1701.

(26) Smith, A. B., III; Hirschmann, R.; Pasternak, A.; Akaishi, R.; Guzman, M. C.; Jones, D. R.; Keenan, T. R.; Sprengler, P. A. Design and Synthesis of Peptidomimetic Inhibitors of HIV-1 Protease and Renin. Evidence for Improved Transport. *J. Med. Chem.* **1994**, *37*, 214–218.

(27) Schechter, I.; Berger, A. On the Size of the Active Site in Proteases. *Biochem. Biophys. Res. Commun.* **1967**, *27*, 157–162.

(28) Gordon, T.; Hansen, P.; Morgan, B.; Singh, J.; Baizman, E.; Ward, S. Peptide Azoles: A New Class of Biologically-Active Dipeptide Mimetics. *BioMed. Chem. Lett.* **1993**, *3*, 915–920.

(29) Miller, M.; Schneider, J.; Sathyanarayana, B. K.; Toth, M. V.; Marshall, G. R.; Clawson, L.; Selk, L.; Kent, S. B.; Wlodawer, A. Structure of Complex of Synthetic HIV-1 Protease with a Substrate-Based Inhibitor at 2.3 Å Resolution. *Science* **1989**, *246*, 1149–1152.

(30) Evans, B. E.; Rittle, K. E.; Homnick, C. F.; Springer, J. P.; Hirshfeld, J.; Veber, D. F. A Stereocontrolled Synthesis of Hydroxyethylene Dipeptide Isosteres Using Novel, Chiral Aminoalkyl Epoxides and γ-(Aminoalkyl) γ-Lactones. *J. Org. Chem.* **1985**, *50*, 4615–4625.

(31) Reiter, L. A. Synthesis of 4(5)-Acyl, 1-Substituted 5-Acyl, and 1-Substituted 4-Acyl-1H-Imidazoles from 4-Aminoisoxazoles. *J. Org. Chem.* **1987**, *52*, 2714.

(32) Attenburrow, J.; Cameron, A. F. B.; Chapman, J. H.; Evans, R. M.; Hems, B. A.; Jansen, A. B. A.; Walker, T. A Synthesis of Vitamin A from Cyclohexanone. *J. Chem. Soc.* **1952**, 1094–1111.

(33) Dreyer, G. B.; Lambert, D. M.; Meek, T. D.; Carr, T. J.; Tomaszek, T. A., Jr.; Fernandez, A. V.; Bartus, H.; Cacciavillani, E.; Hassell, A.; Minnich, M.; Petteway, S. R., Jr.; Metcalf, B. W.; Lewis, M. Hydroxyethylene Isostere Inhibitors of Human Immunodeficiency Virus-1 Protease: Structure-Activity Analysis Using Enzyme Kinetics, X-ray Crystallography, and Infected T-Cell Assays. *Biochemistry* **1992**, *31*, 6646–6659.

(34) Murthy, K. H. M.; Winborne, E. L.; Minnich, M. D.; Culp, J. S.; Debouck, C. The Crystal Structures at 2.2-Å Resolution of Hydroxyethylene-based Inhibitors Bound to Human Immunodeficiency Virus Type 1 Protease Show That the Inhibitors are Present in Two Distinct Orientations. *J. Biol. Chem.* **1992**, *267*, 22770–22778.

(35) Dreyer, G. B.; Boehm, J. C.; Chenera, B.; DesJarlais, R. J.; Hassell, A. M.; Meek, T. D.; Tomaszek, T. A., Jr.; Lewis, M. A Symmetric Inhibitor Binds HIV-1 Protease Asymmetrically. *Biochemistry* **1993**, *32*, 937–947.

(36) Fitzgerald, P. M.; McKeever, B. M.; VanMiddlesworth, J. F.; Springer, J. P.; Heimbach, J. C.; Leu, C. T.; Herber, W. K.; Dixon, R. A.; Darke, P. L. Crystallographic Analysis of a Complex Between Human Immunodeficiency Virus Type 1 Protease and Acetyl-Pepstatin at 2.0-Å Resolution. *J. Biol. Chem.* **1990**, *265*, 14209–14219.

(37) Lespieau, R.; Bourguel, M. 3-cyclohexyl-2-bromopropene. *Organic Syntheses*; Wiley: New York, 1941; Collect. Vol. No. 1, pp 186–187.

(38) Still, W. C.; Kahn, M.; Mitra, A. Rapid Chromatographic Technique for Preparative Separations with Moderate Resolution. *J. Org. Chem.* **1978**, *43*, 2923–2925.

(39) Ratner, L.; Haseltine, W. A.; Patarca, R.; Livak, K. J.; Starcich, B.; Josephs, S. F.; Doran, E. R.; Rafalski, J. A.; Whitehorn, E. A.; Baumeister, K.; Ivanoff, L.; Petteway, S. R.; Pearson, M. L.; Lautenberger, J. A.; Papas, T. K.; Ghrayeb, J.; Chang, N. T.; Gallo, R. C.; Wong-Staal, F. Complete Nucleotide Sequence of the AIDS Virus, HTLV-III. *Nature* **1985**, *313*, 277–284.

(40) Debouck, C.; Gorniak, J. G.; Strickler, J. E.; Meek, T. D.; Metcalf, B. W.; Rosenberg, M. Human Immunodeficiency Virus Protease Expressed in Escherichia coli Exhibits Autoprocessing and Specific Maturation of the gag Precursor. *Proc. Natl. Acad. Sci. U.S.A.* **1987**, *84*, 8903–8906.

(41) Grant, S. K.; Deckman, I. C.; Minnich, M. D.; Culp, J.; Franklin, S.; Dreyer, G. B.; Tomaszek, T. A., Jr.; Debouck, C.; Meek, T. D. Purification and Biochemical Characterization of Recombinant Simian Immunodeficiency Virus Protease and Comparison to Human Immunodeficiency Virus Type 1 Protease. *Biochemistry* **1991**, *30*, 8424–8434.

(42) Strickler, J. E.; Gorniak, J.; Dayton, B.; Meek, T.; Moore, M.; Magaard, V.; Malinowski, J.; Debouck, C. Characterization and Autoprocessing of Precursor and Mature Forms of Human Immunodeficiency Virus Type 1 (HIV 1) Protease Purified From Escherichia coli. *Proteins* **1989**, *6*, 139–154.

(43) Moore, M. L.; Bryan, W. M.; Fakhoury, S. A.; Magaard, V. W.; Huffman, W. F.; Dayton, B. D.; Meek, T. D.; Hyland, L.; Dreyer, G. B.; Metcalf, B. W.; Strickler, J. E.; Gorniak, J. G.; Debouck, C. Peptide Substrates and Inhibitors of the HIV-1 Protease. *Biochem. Biophys. Res. Commun.* **1989**, *159*, 420–425.

(44) Dreyer, G. B.; Metcalf, B. W.; Tomaszek, T. A., Jr.; Carr, T. J.; Chandler, A. C., III; Hyland, L.; Fakhoury, S. A.; Magaard, V. W.; Moore, M. L.; Strickler, J. E.; Debouck, C.; Meek, T. D. Inhibition of Human Immunodeficiency Virus 1 Protease in vitro: Rational Design of Substrate Analogue Inhibitors. *Proc. Natl. Acad. Sci. U.S.A.* **1989**, *86*, 9752–9756.

(45) McPherson, A. J. The Growth and Preliminary Investigation of Protein and Nucleic Acid Crystals for X-Ray Diffraction Analysis. *Methods Biochem. Anal.* **1976**, *23*, 249–345.

(46) Howard, A. J.; Gilliland, G. L.; Finzel, B. C.; Poulos, T. L.; Ohlendorf, D. H.; Salemme, F. R. The Use of an Imaging Proportional Counter in Macromolecular Crystallography. *J. Appl. Crystallogr.* **1987**, *20*, 383–387.

(47) Hendrickson, W. A. Stereochemically Restrained Refinement of Macromolecular Structures. *Methods Enzymol.* **1985**, *115*, 252–270.

(48) Smith, J. L.; Corfield, P. W.; Hendrickson, W. A.; Low, B. W. Refinement at 1.4 Å Resolution of a Model of Erabutoxin b: Treatment of Ordered Solvent and Discreet Disorder. *Acta Crystallogr. A* **1988**, *44*, 357–368.

(49) Jones, T. A. Interactive Computer Graphics: FRODO. *Methods Enzymol.* **1985**, *115*, 157–171.

(50) Brunger, A. T.; Kuriyan, J.; Karplus, M. Crystallographic R Factor Refinement by Molecular Dynamics. *Science* **1987**, *235*, 458–460.

(51) Bernstein, F. C.; Koetzle, T. F.; Williams, G. J.; Meyer, E. E. J.; Brice, M. D.; Rodgers, J. R.; Kennard, O.; Shimanouchi, T.; Tasumi, M. The Protein Data Bank: A Computer-based Archival File for Macromolecular Structures. *J. Mol. Biol.* **1977**, *112*, 535–542.